Analytical Methods

DOI: 10.1002/ange.201405742

Lysosomal pH Rise during Heat Shock Monitored by a Lysosome-Targeting Near-Infrared Ratiometric Fluorescent Probe**

*Qiongqiong Wan, Suming Chen, Wen Shi, Lihong Li, and Huimin Ma**

Abstract: *Heat stroke is a life-threatening condition, featuring a high body temperature and malfunction of many organ systems. The relationship between heat shock and lysosomes is poorly understood, mainly because of the lack of a suitable research approach. Herein, by incorporating morpholine into a stable hemicyanine skeleton, we develop a new lysosome-targeting near-infrared ratiometric pH probe. In combination with fluorescence imaging, we show for the first time that the lysosomal pH value increases but never decreases during heat shock, which might result from lysosomal membrane permeabilization. We also demonstrate that this lysosomal pH rise is irreversible in living cells. Moreover, the probe is easy to synthesize, and shows superior overall analytical performance as compared to the existing commercial ones. This enhanced performance may enable it to be widely used in more lysosomal models of living cells and in further revealing the mechanisms underlying heat-related pathology.*

Heat-related pathologies, such as heat stroke, are one of the most serious causes of mortality.[1] Despite the severity and increasingly prevalent health risks associated with heat-inflicted damage, the molecular and organelle mechanisms responsible for the direct cytotoxicity of heat are not well understood.[2] As one of the vital organelles, the lysosome usually has an acidic environment of pH 3.8–5.0, and plays a key role in cellular homeostasis and the mediation of a variety of physiological processes, such as protein degradation and plasma membrane repair.[3] The minor pH fluctuation of lysosomes may influence these processes and even the fate of the cells.[3a] However, the relationship between temperature change and lysosomal pH value remains unknown. Thus, accurate measurement of the acidity change in lysosomes under heat stress such as heat shock is necessary to gain insight into the mechanism of heat cytotoxicity.

In this respect, fluorescence spectroscopy has attracted significant attention because of its high sensitivity and unrivaled spatiotemporal resolution.[4–10] An excellent fluorescent probe suited for monitoring the quantitative change of lysosomal pH in real time should meet at least three prerequisites: a) it should be lysosome-targeting, b) it should have a long analytical wavelength (greater than $\lambda = 650$ nm or near-infrared) to minimize autofluorescence and biological damage, and c) it should have a reversible pH-dependent ratiometric response to avoid the influence of several variants, such as concentration and optical path length.[7] To our knowledge, a lysosome-targeting fluorescent pH probe with these desired properties is still lacking. The most commonly used ratiometric pH probe for lysosomes is the commercially available probe DND-160, which unfortunately has a rather short excitation wavelength of less than $\lambda = 400$ nm.[8]

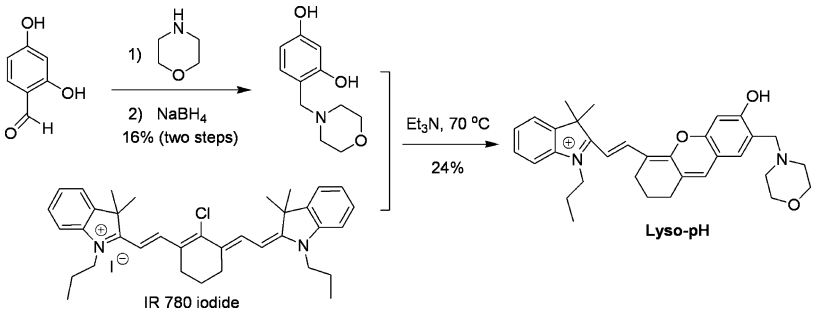

Scheme 1. Synthesis of the lysosome-targeting near-infrared ratiometric fluorescent pH probe Lyso-pH.

With these criteria in mind, we have developed Lyso-pH (Scheme 1 and Scheme S1 in the Supporting Information), a new lysosome-targeting near-infrared ratiometric fluorescent pH probe, by incorporating a typical lysosome-targeting moiety of morpholine[9] into a stable hemicyanine skeleton with near-infrared spectroscopic features. We show that Lyso-pH exhibits an accurate lysosome-targeting ability, excellent photostability, and a good linear ratiometric response in the pH range of 4–6 in living cells. Furthermore, using Lyso-pH-based fluorescence imaging, we find that the lysosomal pH value rises with the increase of temperature, and that this rise in pH is irreversible in living cells. These results demonstrate the relationship between the lysosomal pH value and temperature during heat shock.

[*] Dr. Q. Q. Wan,[+] Prof. Dr. S. M. Chen,[+] Prof. Dr. W. Shi, L. H. Li, Prof. Dr. H. M. Ma
Beijing National Laboratory for Molecular Sciences
Key Laboratory of Analytical Chemistry for Living Biosystems
Institute of Chemistry, Chinese Academy of Sciences
Beijing 100190 (China)
E-mail: mahm@iccas.ac.cn

[+] These authors contributed equally to this work.

[**] This work is supported by grants from the NSF of China (Nos. 21105104, 21275147, and 21321003), 973 Program (No. 2011CB935800), and the Chinese Academy of Science (KJCX2-EW-N06-01 and CMS-PY-201301). We also thank X. Y. Jiang and Z. Huang for help with the CLSM-710 (Carl Zeiss) confocal laser scanning microscope.

Supporting information for this article is available on the WWW under http://dx.doi.org/10.1002/anie.201405742.

Cyanines, a classic type of near-infrared fluorochromes, have been frequently employed to develop different spectroscopic probes for imaging studies, but they are known to have poor stability and high background fluorescence as a result of ready autoxidation and photooxidation.[7a,11] However, hemicyanines, formed from the decomposition of cyanines, usually have high stability, and thus were our first choice to design the stable near-infrared fluorescent pH probe, Lyso-pH. As shown in Scheme 1, the probe Lyso-pH can be easily synthesized by incorporating a lysosome-targeting moiety of morpholine onto the hemicyanine skeleton of the commercially available heptamethine dye, IR 780.

The spectroscopic properties of Lyso-pH were examined in phosphate buffer solution (0.2 M) at different pH values, prepared by varying the relative amounts of Na_2HPO_4, KH_2PO_4, and H_3PO_4. The probe displays sensitive absorption (Figure 1a) and fluorescence (Figure 1b) spectroscopic

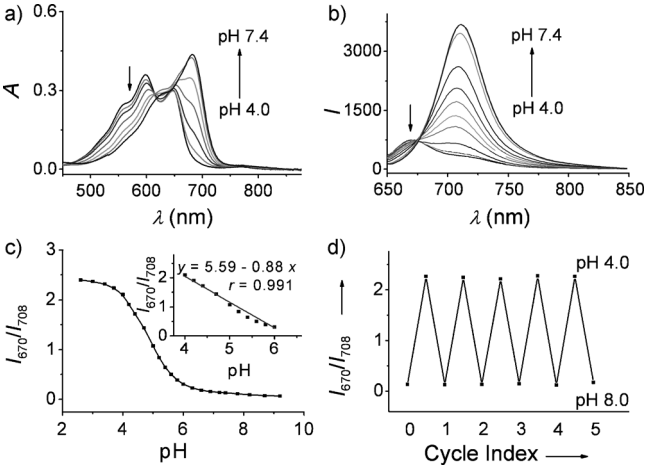

Figure 1. a) Absorption and b) fluorescence emission spectra of Lyso-pH (10 μM) in phosphate buffer (0.2 M) at different pH values. c) Plot of I_{670}/I_{708} (ratio of the fluorescence intensity of Lyso-pH at $\lambda = 670$ nm and $\lambda = 708$ nm) versus pH values in the range pH 2.6–9.2. Inset: the linear relationship between I_{670}/I_{708} and pH values in the range pH 4.0–6.0. d) pH reversibility study of Lyso-pH between pH 4.0 and 8.0. $\lambda_{ex} = 635$ nm; data are expressed as the mean of three separate measurements ± standard deviation (SD).

responses to changes in pH values. As shown in Figure 1a, the maximum absorption band at $\lambda = 598$ nm of the probe in pH 4.0 media is red-shifted to $\lambda = 681$ nm in pH 7.4 media, with a concomitant color change from blue to green (see Figure S5 in the Supporting Information). Upon excitation at $\lambda = 635$ nm, the near-infrared emission intensity at $\lambda = 670$ nm of Lyso-pH decreases slightly with the change in pH values from 4.0 to 7.4. This change in intensity is accompanied by a large increase of fluorescence intensity at $\lambda = 708$ nm (Figure 1b), which provides the basis for achieving a ratiometric (I_{670}/I_{708}) detection. Most notably, the probe Lyso-pH, with a pK_a value of 5.00 ± 0.01 and a quantum yield of $\Phi_f = 0.16$ at pH 5.0, exhibits an excellent I_{670}/I_{708} linearity in the pH range 4.0–6.0 (Figure 1c). The probe shows also good reversibility between pH 4.0 and pH 8.0 (Figure 1d and Figure S6), which is attributed to the protonation/deprotonation of the hydroxy group (Scheme S1). This indicates that the ratiometric response of Lyso-pH matches well with the physiological pH range (pH 3.8–5.0) of lysosomes, making it promising as a near-infrared fluorescent probe for accurate measurement of lysosomal pH values.

We next investigated the specificity of the probe for pH detection over the detection of other biologically relevant species, such as ions, protein, reactive oxygen species, amino acids, and glucose. No obvious change in fluorescence signal was detected in the presence of these species at their physiological concentrations, as compared to the control (Figure S7), indicating that Lyso-pH exhibits high selectivity for pH detection. Moreover, the influence of temperature from 31 °C to 45 °C was examined on the fluorescence of Lyso-pH itself (Figure S8). It is found that changing the temperature within this range does not significantly affect the ratiometric fluorescence signal of Lyso-pH. Additionally, Lyso-pH exhibits good biocompatibility (Figure S9). These results indicate that Lyso-pH may detect changes in lysosomal pH values with minimum interference from temperature and other biologically relevant species.

To evaluate the lysosome-targeting performance of Lyso-pH, HeLa or MCF-7 cells were co-stained with Lyso-pH and LysoTracker Red DND-99 (a commercially available lysosome-targeting dye). As DND-99 is not a ratiometric fluorescence probe, a single channel covering the whole emission wavelength range of DND-99 is selected. For comparison, the corresponding single channel covering the whole emission wavelength range of Lyso-pH is used in this experiment. As shown in Figure 2a, both DND-99 and Lyso-pH display strong localized fluorescence within lysosomes. The fluorescence images of DND-99 and Lyso-pH can be merged rather well, confirming that Lyso-pH can specifically target the lysosomes of living cells with good cell-membrane permeability. Additionally, a high Pearson coefficient of 0.91 and an overlap coefficient of 0.90 are calculated from the intensity correlation plots (Figure 2a, fourth image). Furthermore, there are relatively few changes in the emission intensity profiles of the dyes Lyso-pH and DND-99 (Figure 2c) within the linear region of interest (ROI; given by a yellow line in Figure 2a). Similar results are obtained for HeLa cells (Figure S10a). These results demonstrate the superior lysosome-targeting ability of Lyso-pH. Importantly, this ability of Lyso-pH still holds at the higher temperatures of 41 °C and 45 °C (Figures S11 and S12 in the Supporting Information).

HeLa and MCF-7 cells were also co-stained with Lyso-pH and Rhodamine 123 (a typical mitochondrial tracker). As depicted in Figure 2b, Lyso-pH and Rhodamine 123 lead to the production of bright localized fluorescence within lysosomes and mitochondria, respectively, and the merged image of Lyso-pH and Rhodamine 123 exhibits a significantly different fluorescence (the third image in Figure 2b), which reflects the corresponding lysosomal and mitochondrial distributions. Importantly, not only low values for the Pearson coefficient (0.18) and the overlap coefficient (0.20) are obtained, but also completely different changes in the intensity profile of ROI are found (Figure 2d). Moreover, similar phenomena are found for targeting lysosomes in HeLa cells (Figure S10b).

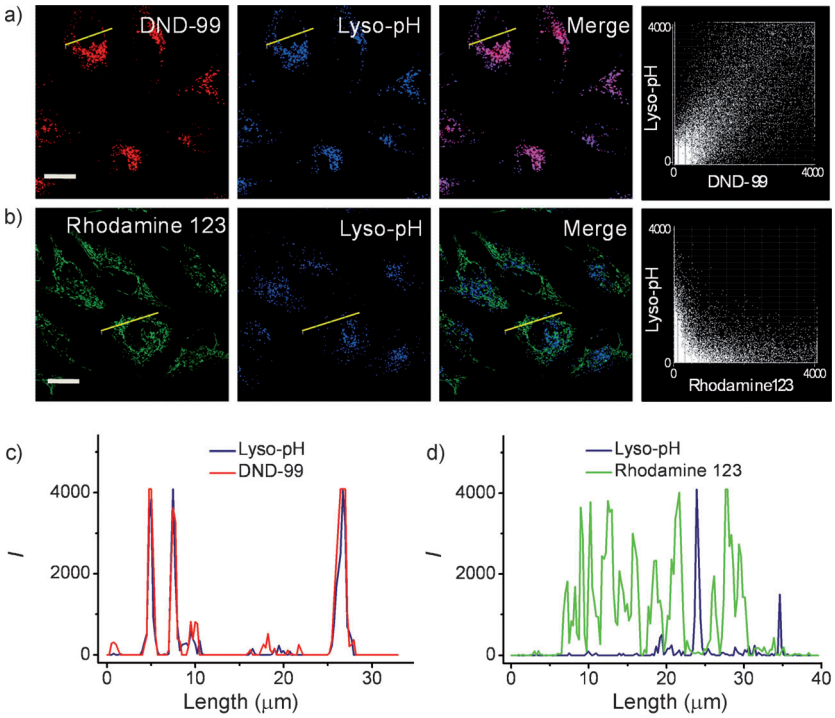

Figure 2. Lysosome-targeting properties of Lyso-pH in MCF-7 cells. a) Colocalization images of MCF-7 cells stained with DND-99 (50 nM, red channel, $\lambda_{ex}=559$ nm, $\lambda_{em}=570$–670 nm) and Lyso-pH (50 nM, blue channel, $\lambda_{ex}=635$ nm, $\lambda_{em}=650$–750 nm), and the correlation of Lyso-pH and DND-99 intensities. b) Colocalization imaging of MCF-7 cells stained with Rhodamine 123 (50 nM, green channel, $\lambda_{ex}=488$ nm, $\lambda_{em}=500$–600 nm) and Lyso-pH (as in (a)), and the correlation of Lyso-pH and Rhodamine 123 intensities. c) Intensity profiles within the ROI (yellow line in Figure 2a) of Lyso-pH and DND-99 across MCF-7 cells. d) Intensity profiles within the ROI (yellow line in Figure 2b) of Lyso-pH and Rhodamine 123 across MCF-cells. Scale bars = 20 μm.

The intracellular photostability of Lyso-pH was also evaluated by comparison with that of DND-99. In this experiment, HeLa cells were successively incubated with DND-99 and Lyso-pH, and the photostability of the two dyes in the cells was compared under a simultaneous continuous excitation by $\lambda=559$ nm and 635 nm lasers.[12] As shown in Figure S13, the fluorescence of DND-99 is bleached quickly in the first 20 minutes, and decreases to about 60% of the initial intensity after 40 minutes. In contrast, the fluorescence of Lyso-pH is rather stable, remaining almost constant (the fluorescence intensity decreases less than 10%) even after 40 minutes of continuous intensive irradiation. This excellent intracellular photostability of Lyso-pH offers great potential for bioimaging applications.

To quantitatively determine lysosomal pH values, the intracellular pH calibration curves of Lyso-pH in both HeLa cells and MCF-7 cells were first made with the antibiotic nigericin as a H^+/K^+ ionophore.[4o,7c] As depicted in Figure S14 for HeLa cells, the fluorescence intensity of the first row (red channel) decreases with a change in the pH value from 4.0 to 6.0, whereas that of the second row (green channel) gradually increases. Additionally, the merged images of red and green channels exhibit distinct pH-dependent patterns. Importantly, the fluorescence intensity ratio ($R=I_{650\text{-}680}/I_{690\text{-}720}$) from the two channels shows a sensitive response to pH change in the range of pH 4.0–6.0 (Figure S16a). This can be described by the linear equation for the fluorescence intensity ratio, $R=4.41$–$0.64\,pH$ ($r=0.995$, where r is the correlation coefficient). In MCF-7 cells, a good linear relationship was also obtained, which can be described by the equation: $R=4.54$–$0.65\,pH$ ($r=0.998$; Figures S15 and S16b).

To investigate the influence of temperature on lysosomal acidity, the dynamic changes of lysosomal pH values in HeLa and MCF-7 cells during heat shock were monitored by confocal fluorescence imaging using Lyso-pH. In this experiment, 41 °C and 45 °C were used as the heat shock temperatures acting on the cells. As shown in Figures 3a,b (see also Figure S17 for more details), when compared to the control group (37 °C) the merged images of the heat-treated cells exhibit obvious color changes (more yellow in color) with the temperature increase, which is attributed to the small increase of the lysosomal pH value. From the constructed pH calibration curves (Figure S16), these pH alterations in lysosomes can be quantitatively determined (Figure 3c). It is found that the normal lysosomal pH values of HeLa and MCF-7 cells (control groups at 37 °C) are 4.58 ± 0.09 and 4.55 ± 0.08, and heat shock at 41 °C causes the increase of their lysosomal pH values to 4.80 ± 0.06 and 4.81 ± 0.07, respectively. Higher temperature treatment at 45 °C further raises their lysosomal pH value to 4.89 ± 0.07 and 4.91 ± 0.08. Although the lysosomal pH differences between 41 °C and 45 °C have no statistical significance, those between 37 °C and 41 °C (or 45 °C) are significant (Figure 3c). Additional control experiments were carried out by first heating the cells to 45 °C and then adding the probe. These experiments show negligible differences from those carried out by adding Lyso-pH to the cells at 37 °C and then heating the cells to 45 °C, illustrated by similar ratio values in both cases (see Figure S18). This also suggests that the probe is stable in cells during the heat treatment from 37 °C to 45 °C. Surprisingly, no decrease in the lysosomal pH value is detected during the heat treatments. This phenomenon may be called unidirectional change (that is, the increase rather than the decrease of the lysosomal pH value induced by heat shock), which is similar to the fact that some diseases lead to an increase rather than a decrease in human body temperature. Moreover, this finding is supported by a comparative study with DND-160 (a commercially available lysosomal pH probe), as shown in Figures S19 and S22. These results clearly indicate that heat shock can lead to an increase of lysosomal pH. The reason for this may be rather complex, but a possible speculation may be made that heat shock might cause the permeabilization of the lysosomal membrane.[13] As a conse-

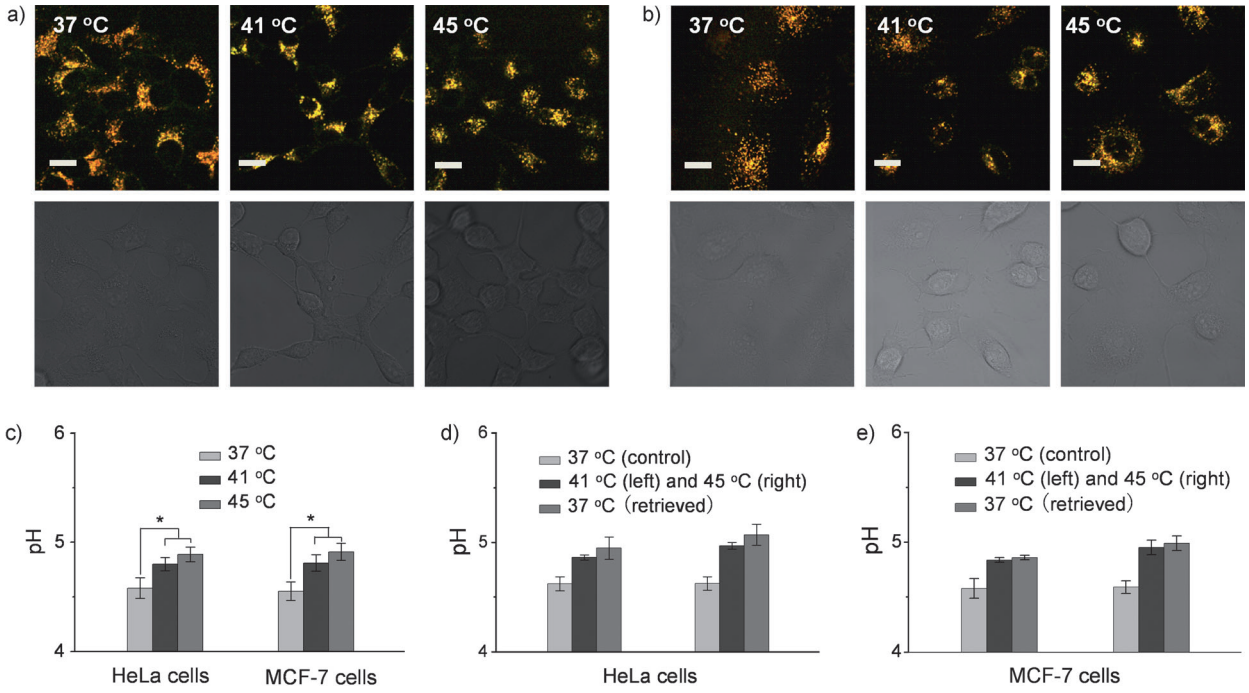

Figure 3. Relationship between lysosomal pH and heat shock in HeLa and MCF-7 cells monitored by Lyso-pH. a), b) The fluorescence images (top, merged; bottom, differential interference contrast) of Lyso-pH-loaded HeLa cells (a) and MCF-7 cells (b) under heat shock at 37 °C, 41 °C, and 45 °C (left to right) for 20 minutes. The fluorescence images are the merged images from both red (λ_{em} = 650–680 nm) and green (λ_{em} = 690–720 nm) channels at λ_{ex} = 635 nm. See also Supporting Information for more details. c) Lysosomal pH changes with temperature in HeLa and MCF-7 cells. The lysosomal pH values in control and heat-treated cells were quantified by image analysis with 100–200 cells counted per condition. Results are expressed as the mean of three separate measurements ± SD. Statistical analyses are performed using the Student's t-test: *P < 0.001. d), e) Reversibility of the lysosomal pH change in HeLa cells (d) and MCF-7 cells (e) with temperature. Results are expressed as the mean of three separate measurements ± SD. Scale bars = 20 μm.

quence, neutralization might occur to some extent between the cytosol, with a higher pH value, and lysosomes, thereby increasing the lysosomal pH.

Furthermore, the analytical performances of Lyso-pH and DND-160 were also compared, which reveals that Lyso-pH has a longer excitation wavelength (λ_{ex} = 635 nm), lower autofluorescence (Figure S21), and higher photostability (comparing Figures S20 and S13) than DND-160 (λ_{ex} = 375 nm). This clearly demonstrates that Lyso-pH is more suitable for lysosomal pH studies.

Finally, the reversibility of the lysosomal pH change in HeLa and MCF-7 cells with temperature was examined in real-time by fluorescence imaging. As depicted in Figure 3d and Figure S23, after the heat-treated HeLa cells at 41 °C and 45 °C are cooled to 37 °C for 20 minutes, their lysosomal pH values are found to be 4.95 ± 0.09 and 5.07 ± 0.10, respectively. These values are much higher than the average value of approximately pH 4.6 from the control groups at 37 °C. For MCF-7 cells, similar results were obtained (Figure 3e and Figure S24). Furthermore, a longer incubation time of 1 hour at 37 °C does not contribute to the recovery of the lysosomal pH (Figure S25). These observations suggest that the lysosomal pH of the heat-treated cells cannot be restored to its initial status, indicating that the rising of lysosomal pH during heat shock is an irreversible process.

In conclusion, on the basis of the relatively stable semicyanine skeleton that is formed from the degradation of IR 780, we have developed a near-infrared ratiometric fluorescent probe, Lyso-pH, for lysosomal pH measurements. The probe can be readily prepared and shows excellent lysosome-targeting ability and high photostability as compared to the existing commercially available probes. More importantly, using our probe Lyso-pH the change of lysosomal pH with temperature is investigated, revealing for the first time the increase of the lysosomal pH during heat shock and the irreversibility of this process. We believe that Lyso-pH may find more applications in detecting pH values in vivo and exploring the function of intracellular acidic lysosomes.

Received: May 29, 2014
Revised: July 29, 2014
Published online: August 22, 2014

Keywords: dyes/pigments · fluorescent probes · heat shock · imaging agents · lysosomal pH

[1] J. A. Patz, D. Campbell-Lendrum, T. Holloway, J. A. Foley, *Nature* **2005**, *438*, 310–317.
[2] N. Kourtis, V. Nikoletopoulou, N. Tavernarakis, *Nature* **2012**, *490*, 213–218.
[3] a) C. Settembre, R. Zoncu, D. L. Medina, F. Vetrini, S. Erdin, T. Huynh, M. Ferron, G. Karsenty, M. C. Vellard, V. Facchinetti,

D. M. Sabatini, A. Ballabio, *EMBO J.* **2012**, *31*, 1095 – 1108; b) B. Turk, V. Turk, *J. Biol. Chem.* **2009**, *284*, 21783 – 21787.

[4] a) B. Dehay, A. Ramirez, M. Martinez-Vicente, C. Perier, M. H. Canron, E. Doudnikoff, A. Vital, M. Vila, C. Klein, E. Bezar, *Proc. Natl. Acad. Sci. USA* **2012**, *109*, 9611 – 9616; b) O. S. Wolfbeis, *Angew. Chem. Int. Ed.* **2013**, *52*, 9864 – 9865; *Angew. Chem.* **2013**, *125*, 10048 – 10049; c) H. Zhang, J. Fan, J. Wang, S. Zhang, B. Dou, X. Peng, *J. Am. Chem. Soc.* **2013**, *135*, 11663 – 11669; d) H. J. Kim, C. H. Heo, H. M. Kim, *J. Am. Chem. Soc.* **2013**, *135*, 17969 – 17977; e) X. H. Li, G. X. Zhang, H. M. Ma, D. Q. Zhang, J. Li, D. B. Zhu, *J. Am. Chem. Soc.* **2004**, *126*, 11543 – 11548; f) X. Duan, Z. Zhao, J. Ye, H. Ma, A. Xia, G. Yang, C. Wang, *Angew. Chem. Int. Ed.* **2004**, *43*, 4216 – 4219; *Angew. Chem.* **2004**, *116*, 4312 – 4315; g) H. N. Kim, W. X. Ren, J. S. Kim, J. Yoon, *Chem. Soc. Rev.* **2012**, *41*, 3210 – 3244; h) H. J. Park, C. S. Lim, J. H. Han, T. H. Lee, H. J. Chun, B. R. Cho, *Angew. Chem. Int. Ed.* **2012**, *51*, 2673 – 2676; *Angew. Chem.* **2012**, *124*, 2727 – 2730; i) M. Schäferling, *Angew. Chem. Int. Ed.* **2012**, *51*, 3532 – 3554; *Angew. Chem.* **2012**, *124*, 3590 – 3614; j) M. Yang, Y. Song, M. Zhang, S. Lin, Z. Hao, Y. Liang, D. Zhang, P. R. Chen, *Angew. Chem. Int. Ed.* **2012**, *51*, 7674 – 7679; *Angew. Chem.* **2012**, *124*, 7794 – 7799; k) P. Rivera-Gil, C. Vazquez-Vazquez, V. Giannini, M. P. Callao, W. J. Parak, M. A. Correa-Duarte, R. A. Alvarez-Puebla, *Angew. Chem. Int. Ed.* **2013**, *52*, 13694 – 13698; *Angew. Chem.* **2013**, *125*, 13939 – 13943; l) D. Asanuma, Y. Takaoka, S. Namiki, K. Takikawa, M. Kamiya, T. Nagano, Y. Urano, K. Hirose, *Angew. Chem. Int. Ed.* **2014**, *53*, 6085 – 6089; *Angew. Chem.* **2014**, *126*, 6199 – 6203; m) A. Chatterjee, J. Guo, H. S. Lee, P. G. Schultz, *J. Am. Chem. Soc.* **2013**, *135*, 12540 – 12543; n) J. Han, K. Burgess, *Chem. Rev.* **2010**, *110*, 2709 – 2728; o) A. Masuda, M. Oyamada, T. Nagaoka, N. Tateishi, T. Takamatsu, *Brain Res.* **1998**, *807*, 70 – 77.

[5] a) M. H. Lee, J. H. Han, J. H. Lee, N. Park, R. Kumar, C. Kang, J. S. Kim, *Angew. Chem. Int. Ed.* **2013**, *52*, 6206 – 6209; *Angew. Chem.* **2013**, *125*, 6326 – 6329; b) G. P. Li, D. J. Zhu, L. Xue, H. Jiang, *Org. Lett.* **2013**, *15*, 5020 – 5023.

[6] a) R. V. Benjaminsen, H. H. Sun, J. R. Henriksen, N. M. Christensen, K. Almdal, T. L. Andresen, *ACS Nano* **2011**, *5*, 5864 – 5873; b) K. J. Zhou, H. M. Liu, S. R. Zhang, X. N. Huang, Y. G. Wang, G. Huang, B. D. Sumer, J. M. Gao, *J. Am. Chem. Soc.* **2012**, *134*, 7803 – 7811.

[7] a) X. H. Li, X. H. Gao, W. Shi, H. M. Ma, *Chem. Rev.* **2014**, *114*, 590 – 695; b) D. Srikun, E. W. Miller, D. W. Domaille, C. J. Chang, *J. Am. Chem. Soc.* **2008**, *130*, 4596 – 4597; c) W. Shi, X. H. Li, H. M. Ma, *Angew. Chem. Int. Ed.* **2012**, *51*, 6432 – 6435; *Angew. Chem.* **2012**, *124*, 6538 – 6541.

[8] a) Z. J. Diwu, C. S. Chen, C. L. Zhang, D. H. Klaubert, R. P. Haugland, *Chem. Biol.* **1999**, *6*, 411 – 418; b) J. Liu, W. N. Lu, D. Reigada, J. Nguyen, A. M. Laties, C. H. Mitchell, *IOVS* **2008**, *49*, 772 – 780.

[9] a) H. B. Yu, Y. Xiao, L. J. Jin, *J. Am. Chem. Soc.* **2012**, *134*, 17486 – 17489; b) L. Wang, Y. Xiao, W. M. Tian, L. Z. Deng, *J. Am. Chem. Soc.* **2013**, *135*, 2903 – 2906.

[10] a) D. Oushiki, H. Kojima, T. Terai, M. Arita, K. Hanaoka, Y. Urano, T. Nagano, *J. Am. Chem. Soc.* **2010**, *132*, 2795 – 2801; b) C. E. Aitken, R. A. Marshall, J. D. Puglisi, *Biophys. J.* **2008**, *94*, 1826 – 1835; c) L. Yuan, W. Y. Lin, S. Zhao, W. S. Gao, B. Chen, L. W. He, S. S. Zhu, *J. Am. Chem. Soc.* **2012**, *134*, 13510 – 13523.

[11] Y. Y. Zhang, W. Shi, X. H. Li, H. M. Ma, *Sci. Rep.* **2013**, *3*, 2830.

[12] H. Shi, X. X. He, Y. Yuan, K. M. Wang, D. Liu, *Anal. Chem.* **2010**, *82*, 2213 – 2220.

[13] N. Fehrenbacher, M. Jaattela, *Cancer Res.* **2005**, *65*, 2993 – 2995.